Inorganic Chemistry

Article

pubs.acs.org/IC

d[1] Oxosulfido-Mo(V) Compounds: First Isolation and Unambiguous Characterization of an Extended Series

Christian J. Doonan,[†] Craig Gourlay,[†,♦] David J. Nielsen,[†] Victor W. L. Ng,[†] Paul D. Smith,[†] David J. Evans,[†] Graham N. George,[§] Jonathan M. White,[†,‡] and Charles G. Young*[,¶]

[†]School of Chemistry and [‡]Bio21 Molecular Science and Biotechnology Institute, University of Melbourne, Victoria 3010, Australia

[§]Department of Geological Sciences, University of Saskatchewan, Saskatoon, Saskatchewan S7N 5E2, Canada

[¶]Department of Chemistry and Physics, La Trobe Institute for Molecular Science, La Trobe University, Melbourne, Victoria 3086, Australia

Supporting Information

ABSTRACT: Reaction of $Tp^{iPr}Mo^{VI}OS(OAr)$ with cobaltocene in toluene results in the precipitation of brown, microcrystalline oxosulfido-Mo(V) compounds, $[CoCp_2][Tp^{iPr}Mo^{V}OS(OAr)]$ ($Cp^- = \eta^5\text{-}C_5H_5^-$, Tp^{iPr-} = hydrotris(3-isopropylpyrazol-1-yl)borate, OAr^- = phenolate or 2-^{s}Bu, 2-^{t}Bu, 3-^{t}Bu, 4-^{s}Bu, 4-Ph, 3,5-^{s}Bu$_2$, 2-CO_2Me, 2-CO_2Et or 2-CO_2Ph derivative thereof). The compounds are air- and water-sensitive and display ν(Mo═O) and ν(Mo┄┄S) IR absorption bands at ca. 890 and 435 cm^{-1}, respectively, 20−40 cm^{-1} lower in energy than the corresponding bands in $Tp^{iPr}MoOS(OAr)$. They are electrochemically active and exhibit three reversible cyclovoltammetric waves ($E(Mo^{VI}/Mo^{V})$ = −0.40 to −0.66 V, $E([CoCp_2]^+/CoCp_2)$ = −0.94 V and $E(CoCp_2/[CoCp_2]^-)$ = −1.88 V vs SCE). Structural characterization of $[CoCp_2][Tp^{iPr}MoOS(OC_6H_4CO_2Et\text{-}2)]\cdot 2CH_2Cl_2$ revealed a distorted octahedral Mo(V) anion with Mo═O and Mo┄┄S distances of 1.761(5) and 2.215(2) Å, respectively, longer than corresponding distances in related $Tp^{iPr}MoOS(OAr)$ compounds. The observation of strong S(1s) → (S(3p) + Mo(4d)) S K-preedge transitions indicative of a d[1] sulfido-Mo(V) moiety and the presence of short Mo═O (ca. 1.72 Å) and Mo┄┄S (ca. 2.25 Å) backscattering contributions in the Mo K-edge EXAFS further support the oxosulfido-Mo(V) formulation. The compounds are EPR-active, exhibiting highly anisotropic (Δg 0.124−0.150), rhombic, frozen-glass spectra with g_1 close to the value observed for the free electron (g_e = 2.0023). Spectroscopic studies are consistent with the presence of a highly covalent Mo┄┄S π^* singly occupied molecular orbital. The compounds are highly reactive, with reactions localized at the terminal sulfido ligand. For example, the compounds react with cyanide and PPh_3 to produce thiocyanate and $SPPh_3$, respectively, and various (depending on solvent) oxo-Mo(V) species. Reactions with copper reagents also generally lead to desulfurization and the formation of oxo-Mo(V) or -Mo(IV) complexes.

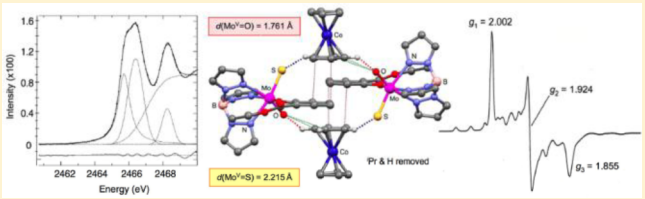

INTRODUCTION

Mononuclear oxosulfido-Mo(V) compounds are extremely rare, intrinsically interesting, and of significant biological relevance. In terms of rarity, there is only one report claiming the isolation of a compound of this type.[1] However, this compound, formulated as $PPh_4[Mo^{V}OS(L\text{-}N_2S_2)]$ ($L\text{-}N_2S_2^{2-}$ = *N*,*N*′-dimethyl-*N*,*N*′-bis(2-mercaptophenyl)ethylenediamine), is unexpectedly air- and water-stable, does not exhibit X-ray absorption spectra or bond distances typical of terminal sulfido ligands,[1−5] and has not been crystallographically characterized. Consequently, we harbor doubts over the veracity of this claim. Certainly, if the compound is an oxosulfido-Mo(V) species, it is very different from the type described herein. Typically, oxosulfido-Mo(V) complexes, including air/water-sensitive $[Mo^{V}OS(L\text{-}N_2S_2)]^-$, are only accessible in situ under sulfidic conditions in dry, deoxygenated solvents (vide infra).[6,7]

Complexes of this type are also intrinsically interesting because they combine "redox incompatible" groups, that is, oxidizing, high-valent oxo-Mo(V) and reducing sulfido groups, and represent relatively stable but otherwise highly reactive metal-thiyl radicals.[8] Notwithstanding their relative stability, extensive delocalization of the unpaired electron onto the sulfido ligand, as revealed by detailed EPR and computational studies (vide infra), predisposes the sulfido ligand to facile reactions. Counterintuitive redox reactions, for example, dimerization, C−H activation/insertion, and induced internal electron-transfer reactions, are among the reactions observed for oxosulfido-Mo(V) and related metal−sulfur compounds.[9,10]

Finally, there is strong evidence that the electron paramagnetic resonance (EPR)-active, "very rapid" form of xanthine oxidase (XnO-VR) contains an oxosulfido-Mo(V) center, namely, $[(MPT)Mo^{V}OS(OR_{urate})]^{2-}$ (MPT = molybdopterin).[11,12] The first direct evidence for this was obtained from multifrequency EPR studies of isotopically labeled (^{n}Mo, ^{17}O, and ^{33}S) enzyme[13−15] and model complexes, including in situ

Received: March 29, 2015
Published: June 5, 2015

DOI: 10.1021/acs.inorgchem.5b00708
Inorg. Chem. 2015, 54, 6386−6396

generated $[MoOS(L\text{-}N_2S_2)]^-$.[14−17] Earlier EXAFS investigations, indicating the presence of an oxosulfido-Mo(VI) in the oxidized enzyme (d(Mo═S) = 2.15−2.25 Å), were consistent with this assignment.[18,19] More recent ESEEM,[20] MCD,[21] ENDOR[22] and crystallographic[23] studies of XnO-VR, along with several computational studies,[24−26] support the presence of a square pyramidal $[(MPT)Mo^{V}OS(OR_{urate})]^{2-}$ center with an apical oxo ligand, a basal sulfido ligand possessing a short Mo⋯S distance of 2.0 ± 0.2 Å, a basal O-bound urate (oxidized substrate), and a bidentate MPT ligand. Oxosulfido-Mo(V) centers are also observed, or are implicated, in the catalytic turnover of other Mo hydroxylases.[11,12] However, a detailed understanding of the electronic structure, behavior, and reactivity of oxosulfido-Mo(V) centers, including their stabilization in biologically relevant dithiolene model complexes and their mechanistic roles during enzyme turnover, inhibition, and deactivation, is yet to be achieved. Accordingly, structural, spectroscopic, and reactivity studies of accessible and relatively stable oxosulfido-Mo(V) model complexes may provide important insights into these rare, unique, and biologically relevant metal centers.

Here, we report the synthesis and characterization of oxosulfido-Mo(V) compounds of the type $[CoCp_2][Tp^{iPr}MoOS(OAr)]$ (Cp^- = η^5-$C_5H_5^-$; Tp^{iPr-} = hydrotris(3-isopropylpyrazol-1-yl)borate, OAr^- = phenolate or derivative thereof; see Chart 1). These compounds represent the first extended series of d^1 oxosulfido-Mo(V) compounds to be isolated and unambiguously characterized. The full description of the synthesis and characterization of the title compounds contained herein follows two brief communications.[2,27]

Chart 1. Compound Structure and Numbering Scheme

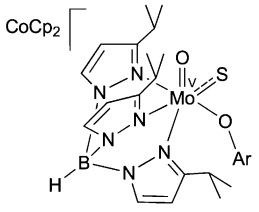

Ar	Cmpd
Ph	1
C_6H_4^{s}Bu-2	2
C_6H_4^{t}Bu-2	3
C_6H_4^{t}Bu-3	4
C_6H_4^{s}Bu-4	5
C_6H_4Ph-4	6
$C_6H_3^{t}Bu_2$-3,5	7
$C_6H_4CO_2$Me-2	8
$C_6H_4CO_2$Et-2	9

EXPERIMENTAL SECTION

Materials and Methods. All reactions were performed under an atmosphere of dinitrogen using standard Schlenk and glovebox techniques and carefully dried and deoxygenated solvents. The starting materials, $Tp^{i}PrMoOS(OAr)$,[4,28] and copper reagents, $[Cu(MeCN)_4]BF_4$,[29] Cu(MeCN)(β-diketiminate) (β-diketiminate = κ^2-HC{C(Me)-N(2,6-$C_6H_3^{i}Pr_2$)}$_2^-$)[30] and [Cu(MeCN)(ttcn)]BF_4 (ttcn = 1,4,7-trithiacyclononane),[31] were prepared according to literature procedures or slight modifications thereof. Commercial samples of cobaltocene (Sigma-Aldrich) were sublimed before use. All other chemicals were reagent grade or above and were used as received.

All spectral and electrochemical data were recorded under anaerobic conditions at ambient temperature (unless otherwise stated). Infrared spectra were recorded on a Biorad FTS 165 FTIR spectrophotometer. Isotropic (295 K) and anisotropic (frozen glass, 110 K) EPR spectra were recorded on a Bruker ECS 106 EPR spectrometer using 1,2-diphenyl-2-picrylhydrazyl as reference, following in situ reduction of $Tp^{iPr}MoOS(OAr)$ with cobaltocene or N^nBu_4SH in 10:1 tetrahydrofuran (THF)/MeCN or toluene. Solutions formed by dissolution of the isolated compounds generally produced poor quality frozen-glasses that yielded broad anisotropic (powder) spectra, whereas in situ generated samples yielded quality glasses and well-resolved spectra (spectral parameters were virtually identical in all cases). EPR simulations and parameter refinements were performed using the WinEPR-SimFonia suite of programs.[32] Cyclic voltammograms were recorded using a 2 mm diameter glassy carbon working electrode, platinum counter-electrode, and a freshly prepared double-jacketed $Ag/AgNO_3$ reference electrode (10 mM $AgNO_3$ in MeCN/0.1 M $N^nBu_4PF_6$ and a clean silver wire) connected to an Autolab Potentiostat operated by the General Purpose Electrochemical System software (version 4.9). Samples were prepared as 1−2 mM solutions in MeCN containing 0.1 M $N^nBu_4PF_6$ as supporting electrolyte. Internal ferrocene was employed to reference potentials to the saturated calomel electrode (+0.400 V vs SCE).[33] Microanalyses were performed by Atlantic Microlabs, Norcross, GA.

Syntheses. The complexes were prepared by the following general procedure. A solution of cobaltocene (0.375 g, 2 mmol) in toluene (10 mL) was added to a stirred solution of $Tp^{iPr}MoOS(OAr)$ (1.5 mmol) in toluene (5 mL). After 20 min, the light brown precipitate that formed was collected by filtration, washed with hexane (5 mL), and dried in vacuo. The compounds were generally pure but retained variable amounts of solvent (removed by pumping under vacuum). Where necessary, samples may be quickly recrystallized from THF/hexane or MeCN/hexane.

$[CoCp_2][Tp^{iPr}MoOS(OPh)]$ ***(1)***. Yield: 757 mg, 66%. Anal. Calcd for $C_{34}H_{43}BCoMoN_6O_2S$: C, 53.34; H, 5.80; N, 10.85; S, 4.15. Found: C, 52.81; H, 5.73; N, 10.85; S, 4.15%. IR (KBr): 3434 br, 3099 m, 2961 m, 2922 w, 2865 m, ν(BH) 2472 m, 2441 m, 1584 m, 1566 w, 1508 s, 1484 s, 1458 m, 1415 m, 1399 m, 1381 m, 1358 m, 1320 w, 1280 m, 1264 m, 1192 s, 1163 w, 1106 m, 1070 m, 1043 s, 1012 m, 966 w, 926 w, 898 sh, ν(Mo═O) 890 m, 858 m, 838 sh, 816 w, 793 m, 774 m, 760 m, 733 s, 695 m, 669 w, 627 m, 596 m, 504 m, 462, ν(Mo⋯S) 440 m cm^{-1}. UV−vis (MeCN), λ, nm (ε, $M^{-1}\cdot cm^{-1}$): 1250 (120), 512 (435).

$[CoCp_2][Tp^{iPr}MoOS(OC_6H_4^{s}Bu\text{-}2)]$ ***(2)***. Yield: 812 mg, 66%. Anal. Calcd for $C_{38}H_{51}BCoMoN_6O_2S$: C, 55.55; H, 6.26; N, 10.23; S, 3.90. Found: C, 55.65; H, 6.20; N, 9.95; S, 3.78%. IR (KBr; cm^{-1}): 3430 br, 3103 m, 2964 s, 2924 m, 2867 m, ν(BH) 2472 w, 2442 m, 1580 w, 1508 s, 1478 s, 1441 m, 1414 m, 1398 m, 1384 m, 1361 m, 1249 m, 1193 s, 1162 w, 1105 m, 1069 m, 1044 s, 1011 m, 927 m, ν(Mo═O) 882 m, 862 m, 836 w, 792 m, 772 m, 735 s, 692 m, 670 w, 627 w, 598 w, 504 w, 461 s, ν(Mo⋯S) 442 m cm^{-1}.

$[CoCp_2][Tp^{iPr}MoOS(OC_6H_4^{t}Bu\text{-}2)]$ ***(3)***. Yield: 837 mg, 68%. Anal. Calcd for $C_{38}H_{51}BCoMoN_6O_2S$: C, 55.55; H, 6.26; N, 10.23; S, 3.90. Found: C, 55.30; H, 6.20; N, 10.59; S, 3.65%. IR (KBr; cm^{-1}): 3436 br, 3107 m, 2960 m, 2922 w, 2865 m, ν(BH) 2472 m, 2442 m, 1586 m, 1508 s, 1477 s, 1457 w, 1414 m, 1396 m, 1384 m, 1358 m, 1292 w, 1279 m, 1268 m, 1192 s, 1157 w, 1127 w, 1100 m, 1088 w, 1069 m, 1041 s, 1013 m, 927 w, 893 s, ν(Mo═O) 876 m, 860 w, 826 w, 792 m, 773 m, 747 m, 732 w, 692 w, 627 w, 611 m, 503 w, 460 m, ν(Mo⋯S) 444 m, 426 m cm^{-1}.

$[CoCp_2][Tp^{iPr}MoOS(OC_6H_4^{t}Bu\text{-}3)]$ ***(4)***. Yield: 874 mg, 71%. Anal. Calcd for $C_{38}H_{51}BCoMoN_6O_2S$: C, 55.55; H, 6.26; N, 10.23; S, 3.90. Found: C, 55.89; H, 6.33; N, 10.09; S, 3.77%. IR (KBr): 3435 br, 3107 m, 2965 s, 2868 m, ν(BH) 2483 m, 1587 m, 1508 s, 1482 w, 1459 w, 1415 m, 1400 w, 1384 m, 1363 m, 1286 m, 1228 w, 1197 s, 1107 w, 1070 m, 1045 s, 1015 m, 937 m, ν(Mo═O) 890 m, 858 m, 817 w, 778 m, 734 s, 701 w, 625 w, 461 m, ν(Mo⋯S) 425 m cm^{-1}.

$[CoCp_2][Tp^{iPr}MoOS(OC_6H_4^{s}Bu\text{-}4)]$ ***(5)***. Yield: 923 mg, 75%. Anal. Calcd for $C_{38}H_{51}BCoMoN_6O_2S$: C, 55.55; H, 6.26; N, 10.23; S, 3.90. Found: C, 55.69; H, 6.16; N, 9.80; S, 4.10%. IR (KBr; cm^{-1}): 3435 br, 3086 m, 2961 s, 2922 m, 2865 m, ν(BH) 2480 m, 2447 m, 1598 m, 1509 s, 1488 m, 1461 m, 1413 m, 1398 m, 1380 m, 1357 m, 1295 w, 1262 s, 1190 s, 1172 w, 1105 m, 1097 w, 1068 m, 1041 s, 1011 m, 954 w, 925 w, ν(Mo═O) 884 s, 860 m, 827 m, 814 w, 791 w, 780 m, 734 s, 695 w, 663 w, 623 w, 586 m, 546 w, 504 w 460 m, ν(Mo⋯S) 437 s cm^{-1}.

$[CoCp_2][Tp^{iPr}MoOS(OC_6H_4Ph\text{-}4)]$ ***(6)***. Yield: 843 mg, 67%. Anal. Calcd for $C_{40}H_{47}BCoMoN_6O_2S$: C, 57.09; H, 5.63; N, 9.99; S, 3.81. Found: C, 56.96; H, 5.52; N, 9.92; S, 3.81%. IR (KBr): 3436 br, 3104

DOI: 10.1021/acs.inorgchem.5b00708
Inorg. Chem. 2015, 54, 6386−6396

Table 1. Selected Distances and Angles for $9{\cdot}2CH_2Cl_2$

distances (Å)			
Mo(1)−O(2)	1.761(5)	Mo(1)−N(21)	2.328(6)
Mo(1)−S(1)	2.215(2)	Mo(1)−N(31)	2.214(5)
Mo(1)−O(1)	2.989(4)	O(1)−C(1)	1.324(7)
Mo(1)−N(11)	2.381(6)	Co−C_{av}[a]	1.998
angles (deg)			
O(2)−Mo(1)−S(1)	107.33(14)	S(1)−Mo(1)−N(31)	92.19(14)
O(2)−Mo(1)−O(1)	100.89(18)	O(1)−Mo(1)−N(11)	84.49(18)
O(2)−Mo(1)−N(11)	161.15(19)	O(1)−Mo(1)−N(21)	84.30(18)
O(2)−Mo(1)−N(21)	86.56(18)	O(1)−Mo(1)−N(31)	163.70(19)
O(2)−Mo(1)−N(31)	89.8(2)	N(11)−Mo(1)−N(21)	75.94(19)
S(1)−Mo(1)−O(1)	96.22(14)	N(11)−Mo(1)−N(31)	81.6(2)
S(1)−Mo(1)−N(11)	89.83(14)	N(21)−Mo(1)−N(31)	84.13(18)
S(1)−Mo(1)−N(21)	165.66(14)	C(1)−O(1)−Mo(1)	137.8(4)

[a]Mean Co−C distance in the $[CoCp_2]^+$ cation.

m, 2963 m, 2925 w, 2867 m, ν(BH) 2481 m, 1596 m, 1511 s, 1481 s, 1460 w, 1414 m, 1398 m, 1382 m, 1360 m, 1282 m, 1274 m, 1192 s, 1169 w, 1105 m, 1070 m, 1045 s, 1016 m, ν(Mo═O) 884 m, 858 m, 837 sh, 791 m, 781 m, 766 m, 734 s, 701 m, 646 w, 622 w, 597 m, 505 w, 461 m, ν(Mo═S) 437 m cm^{-1}.

*[$CoCp_2$][$Tp^{iPr}MoOS(OC_6H_3{}^tBu_2$-3,5)] (**7**).* Yield: 822 mg, 60%. Anal. Calcd for $C_{42}H_{59}BCoMoN_6O_2S$: C, 57.47; H, 6.78; N, 9.57; S, 3.65. Found: C, 57.42; H, 6.65; N, 9.92; S, 3.60%. IR (KBr): 3435 br, 3106 m, 2966 w, 2868 m, ν(BH) 2478 m, 2449 m, 1585 m, 1509 s, 1492 w, 1459 w, 1415 m, 1398 m, 1383 m, 1363 m, 1311 m, 1226 w, 1193 s, 1106 m, 1070 m, 1043 s, 1000 m, 975 m, ν(Mo═O) 902 m, 858 m, 817 w, 792 w, 782 m, 775 m, 734 s, 710 w, 643 w, 628 w, 458 m, ν(Mo═S) 425 m cm^{-1}.

*[$CoCp_2$][$Tp^{iPr}MoOS(OC_6H_4CO_2Me$-2)] (**8**).* Yield: 839 mg, 68%. Anal. Calcd for $C_{36}H_{45}BCoMoN_6O_4S$: C, 52.50; H, 5.51; N, 10.21; S, 3.89. Found: C, 52.21; H, 5.48; N, 9.77; S, 4.13%. IR (KBr, cm^{-1}): 3092 w, 3061 w, 2959 w, 2944, w, 2922 w, 2864 w, ν(BH) 2475 w and 2446 w, ν(C═O) 1676 s, 1592 s, 1549 w, 1510 s, 1472 s, 1454 s, 1430 w, 1414 m, 1397 m, 1379 m, 1359 m, 1325 s, 1264 s, 1220 m, 1195 vs, 1158 m, 1126 m, 1105 w, 1068 m, 1041 vs, 1011 m, ν(Mo═O) 888 vs, 875 s, 808 w, 793 m, 775 s, 760 s, 731 vs, 695 m, 659 m, 629 m, 600 s, 568 w, 453 w, 501 w, 461 s, ν(Mo═S) 434 vs.

*[$CoCp_2$][$Tp^{iPr}MoOS(OC_6H_4CO_2Et$-2)] (**9**).* Yield: 904 mg, 72%. Anal. Calcd for $C_{37}H_{47}BCoMoN_6O_4S$: C, 53.06; H, 5.66; N, 10.04; S, 3.83. Found: C, 52.77; H, 5.76; N, 9.75; S, 3.76%. IR (KBr, cm^{-1}): 3105 w, 3061 w, 2960 w, 2924 w, 2899 w, 2865 w, ν(BH) 2475 w and 2446 w, ν(C═O) 1669 s, 1592 m, 1550 w, 1509 s, 1470 vs, 1452 s, 1414 m, 1397 m, 1379 m, 1361 m, 1322 s, 1303 s, 1263 s, 1223 s, 1195 vs, 1159 m, 1129 s, 1096 w, 1068 m, 1041 vs, 1013 m, ν(Mo═O) 888 vs, 862 s, 832 m, 816 m, 793 m, 775 s, 761 s, 732 vs, 694 w, 658 m, 628 m, 602 s, 573 w, 542 w, 501 w, 460 s, ν(Mo═S) 435 vs.

Molybdenyl Species: $Tp^{iPr}MoO(OSAr')$ ($OSAr'^{2-}$ = κ^2-O,S-2-mercaptophenolate derivative). Complexes of this type are known to be produced as the thermodynamic products in the kinetic syntheses of $Tp^{iPr}MoOS(OAr)$ species.[4] They were also observed in reactivity studies involving the title compounds. Additional derivatives were prepared to obtain spectral data for identification purposes. The synthetic procedure and spectral data for these compounds are contained in the Supporting Information.

Reactivity Studies. *Reactions with Cyanide.* In a typical experiment [$CoCp_2$][$Tp^{iPr}MoOS(OAr)$] (20 mg, 0.022−0.026 mmol) and KCN or NEt_4CN (0.088−0.104 mmol) were dissolved in dichloromethane or 10:1 THF/MeCN and stirred at ambient temperature. The progress of the reactions was monitored by EPR and mass spectrometry at intervals. Detection of thiocyanate was achieved by mixing the reaction mixture with threefold excess of Sorbo's reagent,[34] then stirring for 5 min in the absence of light before using UV−visible spectroscopy to detect the absorbance at 460 nm.

Reactions with Triphenylphosphine. In a typical experiment [$CoCp_2$][$Tp^{iPr}MoOS(OAr)$] (20 mg, 0.022−0.026 mmol) and PPh_3 (0.088−0.104 mmol) were dissolved in dichloromethane or 10:1 THF/MeCN and stirred at ambient temperature. Reactions were monitored by EPR and mass spectrometry at 5 min intervals until no changes were observed. Detection of $SPPh_3$ was achieved by ^{31}P NMR.

Reactions with Copper Species. In a typical experiment [$CoCp_2$]-[$Tp^{iPr}MoOS(OAr)$] (20 mg, 0.022−0.026 mmol) and CuL (L = Cl, β-diketiminate) or $[Cu(MeCN)_4]BF_4$ (~0.03 mmol) were dissolved in dichloromethane or 10:1 THF/MeCN and stirred at ambient temperature. Reactions were monitored by EPR and mass spectrometry at 5 min intervals until no changes were observed.

X-ray Crystallography. Brown crystals of $9{\cdot}2CH_2Cl_2$ were grown by diffusion of diethyl ether into a dichloromethane/acetonitrile solution of the complex. Diffraction data were collected to $2\theta = 55°$ on an Oxford XCalibur diffractometer at 130 K using Cu Kα radiation (1.541 84 Å). Cell parameters and data reduction were performed on the Cysallis software. The structure was solved by direct methods (SHELXS-97[35]) and refined using full-matrix least-squares on F^2 (SHELXL-97).[36] Molecular diagrams were generated using ORTEP 3[37] and Mercury[38,39] software. All non-hydrogen atoms were included in difference maps, and anisotropic parameters were employed. Hydrogen atoms were included in calculated positions. Selected bond distances and angles are presented in Table 1.

X-ray Absorption Spectroscopy. Sulfur K-edge X-ray absorption studies were performed at the Stanford Synchrotron Radiation Lightsource (SSRL) with the SPEAR storage ring containing 60−100 mA at 3.0 GeV. Experiments were performed on Beamline 6−2 using an Si(111) double crystal monochromator and a wiggler field of 1.0 T. Harmonic rejection was accomplished using a flat nickel-coated mirror downstream of the monochromator effecting a cutoff energy of 4500 eV. Incident X-ray intensity was monitored using an ion chamber contained in a (flowing) helium-filled flight path. Energy resolution was optimized by decreasing the vertical aperture upstream of the monochromator and quantitatively determined to be 0.51 eV by measuring the width of the 2471.4 eV 1s → π^* 3(b_1) transition of gaseous SO_2, which corresponds to a transition to a single orbital, rather than to a band of orbitals (in contrast to solid standards).[40] X-ray absorption was monitored by recording total electron yield, and the energy scale was calibrated with reference to the lowest energy peak of the sodium thiosulfate standard ($Na_2S_2O_3{\cdot}5H_2O$) which was assumed to be 2469.2 eV.[41] Solutions were prepared in acetonitrile (ca. 100 mM) and examined at ambient temperature. Preedge features were estimated by curve-fitting to a sum of pseudo-Voigt peaks using the program EDG_FIT (pseudo-Voigt deconvolution).[42]

Molybdenum K-edge X-ray absorption spectra were collected on beamline 7−3 using a Si(220) double crystal monochromator with an upstream vertical aperture of 1 mm and a wiggler field of 1.8 T. Harmonic rejection was accomplished by detuning one monochromator crystal to ~60% off-peak. An Oxford Instruments CF1208 continuous-flow liquid helium cryostat maintained a constant sample temperature of 10 K. Spectra were recorded in transmittance mode

DOI: 10.1021/acs.inorgchem.5b00708
Inorg. Chem. 2015, 54, 6386−6396

using argon-filled ionization chambers. A spectrum of molybdenum foil was collected simultaneously with that of the sample, and spectra were calibrated with reference to the lowest energy inflection point of the K-edge, assigned to be 20 003.9 eV. Solid samples were diluted by grinding with boron nitride to give samples with maximum absorbances of ~2.0. Data were analyzed using the EXAFSPAK suite of computer programs (http://ssrl.slac.stanford.edu/EXAFSPAK.html), and no smoothing or related operations were performed on the data.

RESULTS AND DISCUSSION

Synthesis and Characterization. Reaction of $Tp^{iPr}MoOS(OAr)$ with excess cobaltocene in dry, deoxygenated toluene resulted in the rapid precipitation of crystals of $[CoCp_2][Tp^{iPr}MoOS(OAr)]$ in moderate–high yields. These compounds are the kinetic products of the reaction; the thermodynamic products, obtained after prolonged reaction times, generally contain bidentate κ^2-*O,S*-donor mercaptophenolate ligands formed by reaction of the sulfido ligand with the phenolate ring (this behavior is similar to that observed in the synthesis of $Tp^{iPr}MoOS(OAr)$[4]). The brown or red-brown compounds were soluble in THF and acetonitrile and insoluble in toluene, diethyl ether, and hexane. Solutions of the compounds were highly air- and moisture-sensitive, but solid samples could be handled very briefly in air without apparent decomposition; refrigeration is required for long-term storage of the compounds. EPR experiments showed that $[CoCp_2][Tp^{iPr}MoOS(OC_6H_4CO_2Ph\text{-}2)]$ was generated in situ; however, the compound was unstable, and attempted isolation led to the formation of $[CoCp_2][Tp^{iPr}MoO(OC_6H_4SC(O)\text{-}2\text{-}\kappa^2O,S)]$.[27] Correct microanalyses were obtained for all compounds.

The IR spectra of the compounds (Table 2) showed bands characteristic of the Tp^{iPr-} (ν(BH) ca. 2475, ν(CN) 1509 cm^{-1}) and terminal oxo and sulfido ligands. The ν(Mo=O) band appeared in the 902–876 cm^{-1} region, considerably lower in energy than is typical of mono-oxo species and ca. 20–30 cm^{-1} lower than ν(Mo=O) in the $Tp^{iPr}MoOS(OAr)$ precursors. The ν(Mo---S) band appeared in the region of 444–425 cm^{-1}, ~40 cm^{-1} lower than the corresponding bands in $Tp^{iPr}MoOS(OAr)$. These observations are consistent with a weakening of the Mo=O and Mo=S bonds through population of the predominantly Mo---S π^* singly occupied molecular orbital (SOMO) upon one-electron reduction. Both the ν(Mo=O) and ν(Mo---S) modes are sensitive to the nature of the coligand, spanning ranges of 26 and 19 cm^{-1}, respectively, consistent with the involvement of phenolate O-donor p orbitals in the π orbital manifold. Bands characteristic of the cobaltocenium cation (ca. 3098, 1414, 858, and 460 cm^{-1}) are also observed.[43]

Table 2. Comparison of IR Data (cm^{-1})

cmpd number, Ar	ν(Mo=O)	ν(Mo---S)	ν(BH)	ν(CN)
1, Ph	890	440	2472	1508
2, $C_6H_4{}^sBu$-2	882	442	2472	1508
3, $C_6H_4{}^tBu$-2	876	444	2472	1508
4, $C_6H_4{}^tBu$-3	890	425	2483	1508
5, $C_6H_4{}^sBu$-4	884	437	2480	1509
6, C_6H_4Ph-4	884	437	2481	1511
7, $C_6H_3{}^tBu_2$-3,5	902	425	2478	1509
8, $C_6H_4CO_2Me$-2	888	434	2475	1510
9, $C_6H_4CO_2Et$-2	888	435	2475	1509

The cyclic voltammograms of the compounds displayed three reversible waves assignable to Mo^{VI}/Mo^{V} (see Table 3), $[CoCp_2]^+/CoCp_2$ (E = −0.94 V), and $CoCp_2/[CoCp_2]^-$ (E = −1.88 V) couples. The reversible, one-electron Mo^{VI}/Mo^{V} processes occurred from ca. −0.40 to −0.66 V, close to the values derived from electrochemical studies of the Mo(VI) analogues.[4,28] The potentials of these processes vary with the phenolate coligand and have been shown to correlate with Hammett–Smith parameters.[44] The Mo^{VI}/Mo^{V} couples were ca. 300 mV more positive than the corresponding couples exhibited by the dioxo analogues, consistent with the lower energy of the SOMO (due to the reduced ligand field) in the oxosulfido- versus dioxo-Mo complexes. Consequently, the oxosulfido-Mo(V) complexes are easier to produce (thermodynamically) and more difficult to oxidize than their dioxo-Mo(V) counterparts, the latter being the stronger of the two reducing agents, that is, more easily oxidized to Mo(VI).

Table 3. Cyclic Voltammetric Data for the Mo^{VI}/Mo^{V} Couple[a]

cmpd number, Ar	$E_{1/2}$ (V)	ΔE_{pp} (mV)	I_{pa}/I_{pc}
1, Ph	−0.485	83	1.04
2, $C_6H_4{}^sBu$-2	−0.550	130	1.01
3, $C_6H_4{}^tBu$-2	−0.658	98	1.03
4, $C_6H_4{}^tBu$-3	−0.514	96	1.03
5, $C_6H_4{}^sBu$-4	−0.500	107	1.04
6, C_6H_4Ph-4	−0.396	101	1.05
7, $C_6H_3{}^tBu_2$-3,5	−0.542	89	1.02
8, $C_6H_4CO_2Me$-2	−0.462	112	1.03
9, $C_6H_4CO_2Et$-2	−0.475	94	1.03

[a]Recorded in acetonitrile (see Experimental Section). Data for scan rates of 100 mV s^{-1}, with $E_{1/2}$ vs SCE using ferrocene (Fc) as internal standard ($\Delta E_{pp} \approx 75$ mV and $I_{pa}/I_{pc} \approx 1.02$ for Fc/Fc^+).

X-ray Crystallography. Crystallographic characterization of the compounds proved extremely difficult due to persistent oxo/sulfido ligand disorder or competitive decomposition during slow crystal growth. Diffraction studies of disordered crystals confirmed the presence of discrete $[CoCp_2]^+$ and $[Tp^{iPr}MoOS(OAr)]^-$ ions but provided unreliable metrical parameters for the oxo/sulfido ligands. Oxo/sulfido ligand disorder has been observed for many related Mo(VI) and W(VI) compounds, for example, $(\eta^5\text{-}C_5Me_5)MoOS(CH_2SiMe_3)$,[45] $MOS(OSiPh_3)_2(Me_4phen)$ (M = Mo,[46] W;[47] Me_4phen = 3,4,7,8-tetramethyl-1,10-phenanthroline), $Tp^{iPr}MoOS(OAr)$,[4] and Tp*WOSX (Tp^{*-} = hydrotris(3,5-dimethylpyrazol-1-yl)borate, X^- = monoanion).[48] Finally, an acceptable structure, the first for an oxosulfido-Mo(V) compound, was obtained for **9**·$2CH_2Cl_2$. The structure has been communicated,[27] and only key results are reiterated here.

The distorted octahedral anion (shown with its cobaltocenium counterion in Figure 1) exhibits an Mo=O distance of 1.761(5) Å, to the high end of the range typical of Mo=O bonds (1.65–1.85 Å, average (av) 1.706 Å with standard deviation (SD) 0.079 Å[49,50]). A lengthening of this bond is consistent with the weakening observed by IR spectroscopy; a Mo=O distance of 1.75 Å is estimated using the isolated harmonic oscillator approximation[51] and Badger's Rule.[52] The Mo---S bond length of 2.215(2) Å in **9** is also significantly longer than those of $Tp^{iPr}MoOS(OC_6H_4{}^sBu)$ (2.132(2) Å)[4]

DOI: 10.1021/acs.inorgchem.5b00708
Inorg. Chem. 2015, 54, 6386–6396

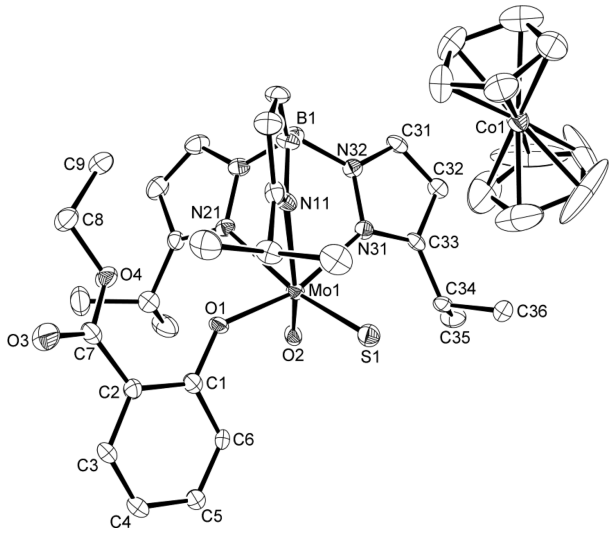

Figure 1. ORTEP projection of the ions in **9**·2CH_2Cl_2 drawn at 30% ellipsoid probability. Lattice solvent molecules and hydrogen atoms were omitted for the sake of clarity.

and related sulfido-Mo complexes (av 2.154 Å with SD 0.087 Å[50]). This bond lengthening results from the occupation of the Mo═S π^*-orbital, which weakens the Mo═S bond as revealed by IR spectroscopy; here, an Mo---S distance of 2.25 Å is estimated using Badger's Rule.[51,52] The O═Mo---S angle of 107.33(14)° is also greater than that of Tp^{iPr}MoOS-($OC_6H_4{}^sBu$) (103.7(2)°),[4] consistent with trends observed in dioxo-Mo(VI) and -Mo(V) complexes.[53,54] Significantly, the Mo---S bond in **9** is much shorter than that reported for PPh_4[MoOS(L-N_2S_2)] (2.36 Å by EXAFS)[1] but close to the range established for XnO-VR (2.0 ± 0.2 Å).[23]

The ions are associated by a variety of interionic interactions, including nonclassical hydrogen bonds and $\pi-\pi$ interactions, to form the dimeric unit shown in Figure 2. These include two short, interionic [$CoCp_2$]$^+$···O═Mo interactions, with H···O distances of 2.42(5) Å and 2.84(4) Å, the stronger interaction being significantly shorter than the sum of the van der Waals radii ($\sum_{OH}$ = 2.65 Å[55]). The thermal ellipsoid of the oxo ligand

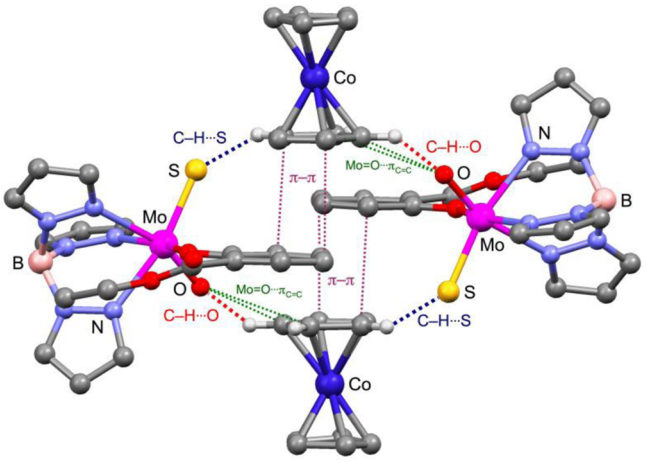

Figure 2. Dimer unit of **9**·2CH_2Cl_2 showing interionic interactions. Isopropyl groups, solvent molecules, and nonparticipating H atoms were excluded for the sake of clarity. Atom colors: Mo (magenta); Co (dark blue); O (red); S (yellow); N (blue); B (pink); C (gray).

is also directed toward the C–H group. These metrical and thermal parameters are indicative of stabilizing C–H···O H-bonds.[56−58] A red shift in the ν(C–H) modes of [$CoCp_2$]$^+$ is also indicative of the presence of these interactions.[59] A single, interionic C–H···S---Mo H-bond interaction is also present in the dimer unit, the H···S distance being 2.66(2) Å and inside the sum of the van der Waals radii ($\sum_{SH}$ = 2.88 Å[55]). Significant $\pi-\pi$ interactions (d_{CC} < 3.3 Å) between the Cp and phenolate rings are also observed. The aforementioned interactions play a major role in the positional ordering of the oxo and sulfido ligands.

X-ray Absorption Spectroscopy. Sulfur K-edge X-ray absorption near-edge spectroscopy (XANES) and Mo K-edge extended X-ray absorption fine structure (EXAFS) experiments (on selected derivatives) provided additional evidence for the oxosulfido-Mo(V) formulation and the presence of a short Mo---S bond, as well as insights into the electronic structure of the compounds. The solution and solid-state S K-edge X-ray absorption spectra of **1** are shown in Figure 3; virtually identical

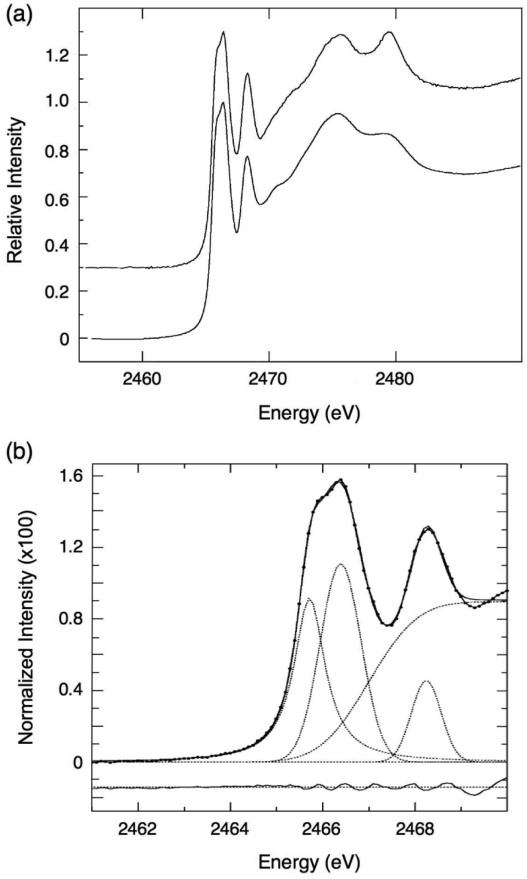

Figure 3. (a) S K-edge X-ray absorption spectra of **1** in solid (upper) and solution (lower) states. (b) Pseudo-Voigt peak fit of the preedge features in the spectrum shown in (a) (solid) with resultant residual (lower trace).

spectra were obtained for **7** (not shown). The spectra exhibit strong, preedge features at 2465.7, 2466.3, and 2468.3 eV with relative integrated intensities and full widths at half-maximum absorption (fwhm (eV) in parentheses) of 0.84 (0.40), 1.0 (0.52), and 0.30 (0.38), respectively. These bands are assigned to S(1s) → (S(3p) + Mo(4d)) transitions, and the observation of them provides incontrovertible evidence for the presence of

DOI: 10.1021/acs.inorgchem.5b00708
Inorg. Chem. 2015, 54, 6386−6396

a terminal sulfido ligand in the title compounds.[1−5] For transitions into an empty orbital, for example, in d^0 Mo(VI) complexes, the relative intensities would be directly proportional to the S(3p) atomic orbital coefficient in the linear combination of atomic orbitals expansion of the formally Mo(4d) orbitals. However, a reduction in the intensity (by ca. half) of the lowest energy band in **1** and **7** is expected due to the reduced probability of a transition into a (formally d^1) SOMO. Thus, although there is significant sulfur character mixed into all the higher energy Mo d orbitals, the sulfur character appears to be greatest for the lowest energy orbital, assigned as the ψ_{xy} π^* SOMO. Finally, the peak widths are consistent with each band corresponding to a single transition, as calibrated by Shadle et al.[60] Analogous bands and interpretations were reported for the S K-edge XANES of monomeric $Tp^{iPr}MoOS(OAr)$ species, the lowest energy band being the most intense for these compounds; for example, $Tp^{iPr}MoOS(OPh)$ exhibits peaks at 2465.9 (relative intensity (I) = 1), 2467.1 (I = 0.48), and 2469.1 (I = 0.44) eV,[5] while $Tp^{iPr}MoOS(OC_6H_4{}^sBu\text{-}2)$ exhibits peaks at 2465.9 (I = 1), 2466.9 (I = 0.51), and 2468.8 (I = 0.35) eV. The highly covalent nature of the interaction revealed by this spectroscopic technique is consistent with EPR studies demonstrating high covalency and spin delocalization from Mo to S in XnO-VR.[13,14]

Analysis of the Mo K-edge EXAFS of **1** and **7** confirmed the presence of terminal oxo and sulfido ligands with Mo═O and Mo⋿S distances of ca. 1.72 and 2.24 Å, respectively. The EXAFS Fourier transform of **1** (Figure 4) displayed overlapping features at ca. 2 Å attributable to a combination of Mo═O, Mo⋿S, Mo−O, and Mo−N backscatterers (an approximate determination of the Mo−N shell was applied due to the high static variation in individual Mo−N distances). Features at ca. 3 Å corresponded to nonbonding N and C atoms of the Tp^{iPr} ligand.[61] The parameters obtained from curve fitting analysis of both compounds are presented in Table 4. The Mo═O distances and associated ν(Mo═O) frequencies (1.73 Å and 890 cm^{-1} for **1**, 1.69 Å and 902 cm^{-1} for **7**) are consistent with the presence of a weaker Mo═O bond in **1** compared to that of **7**. The lower ν(Mo═O) frequency for **9** (888 cm^{-1}) would suggest a further lengthening of the Mo═O bond, consistent with the value obtained by X-ray crystallography (vide supra). The variation in the Mo═O distances of **1**, **7**, and **9** may reflect the extent of lattice interactions involving the oxo group (vide supra). The Mo⋿S distances in Table 4 also correlate with ν(Mo⋿S) values and their bond strength implications (2.23 Å and 440 cm^{-1} for **1**, 2.25 Å and 425 cm^{-1} for **7**). Comparison of data from **7** and **9** is invalidated by the statistically insignificant differences in the comparison data (see footnote to Table 4). Importantly, the Mo⋿S bonds of **1**, **7**, and **9** are all significantly longer than those of related oxosulfido-Mo(VI) species (2.13−2.15 Å[2,4]), consistent with a weakening of the Mo═S bond due to the partial occupation of the Mo⋿S π^* SOMO.

The X-ray absorption spectra of the title compounds are strikingly different than those reported for $PPh_4[MoOS(L\text{-}N_2S_2)]$.[1] This compound does not exhibit the S K-pre-edge transitions[1−5] or the short Mo⋿S distance typical of terminal sulfido compounds (the EXAFS derived Mo−S distances for the compound were ca. 2.36 Å[1] compared to av 2.154 Å[50] for sulfido-Mo compounds and 2.215 Å for **9**). Insights into the true nature of $PPh_4[MoOS(L\text{-}N_2S_2)]$ and/or the origins of its unexpected spectroscopic properties must await further characterization of this compound.

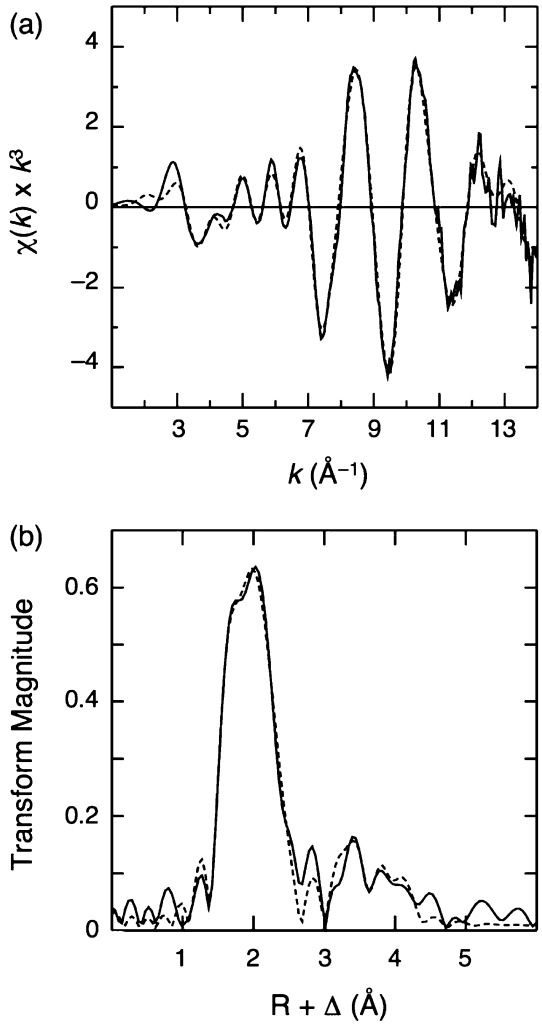

Figure 4. (a) Molybdenum K-edge EXAFS of **1**. (b) Fourier transform of spectrum in (a).

Table 4. EXAFS Curve Fitting Analysis for 1 and 7[a]

cmpd	number/ligand	R (Å)	σ^2 (Å^2)
1	1 Mo═O	1.73	0.0019(1)
	1 Mo−O	2.01	0.0029(2)
	1 Mo⋿S	2.23	0.0021(1)
	3 Mo−N	2.31	0.0064(9)
7	1 Mo═O	1.69	0.0024(1)
	1 Mo−O	2.01	0.0027(4)
	1 Mo⋿S	2.25	0.0023(1)
	3 Mo−N	2.32	0.0068(9)

[a]The parameters for curve fitting are backscatterer (atom type); coordination number N; interatomic distance R; (thermal and static) mean-square deviation in R (the Debye−Waller factor) σ^2. The values in parentheses are estimated standard deviations (precisions) obtained from the diagonal elements of the covariance matrix. We note that the accuracies will be somewhat larger than the precisions (not quoted), typically 0.02 Å for R and 20% for N and σ^2.

Electron Paramagnetic Resonance Spectroscopy. The title compounds are paramagnetic and give rise to strong EPR signals typical of d^1 oxosulfido-Mo(V) species (Figure 5 and Table 5), including the best characterized example, in situ-

DOI: 10.1021/acs.inorgchem.5b00708
Inorg. Chem. 2015, 54, 6386−6396

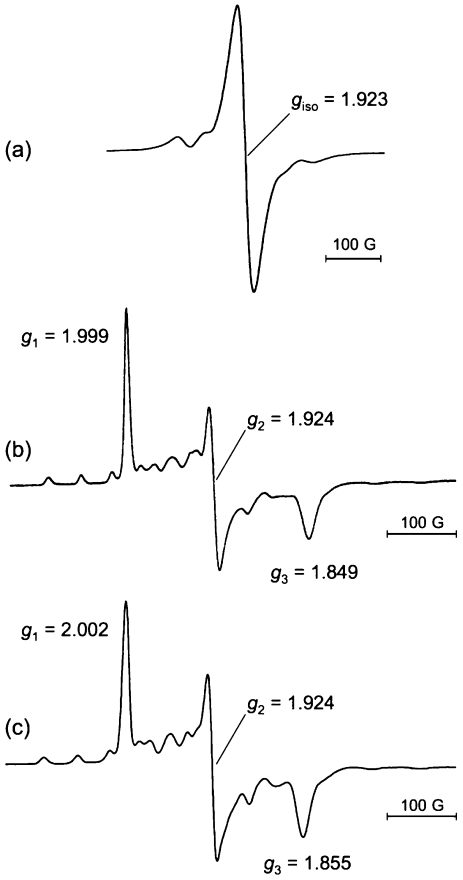

Figure 5. Typical EPR spectra. (a) Isotropic spectrum of **9** in 10:1 THF/MeCN. (b) Frozen-glass spectrum of **1** generated in situ using N^nBu_4SH in toluene. (c) Frozen-glass spectrum of **6** generated in situ using N^nBu_4SH in toluene.

generated $[MoOS(L\text{-}N_2S_2)]^-$.[14−17] Solution EPR spectra were characterized by a broad ($W_{1/2}$ > 20 G) signal with $g_{iso} \approx 1.925$ (Figure 5a). The dominant central feature is associated with Mo isotopomers with nuclear spins $I = 0$ (natural abundance = 75%), while the six satellite peaks are due to hyperfine coupling to ^{95,97}Mo nuclei ($I = 5/2$, 25%). The inner and low-g satellite peaks were often obscured or broadened due to overlap with the broad central peak or the effects of g and A strain. The frozen-glass EPR spectra were rhombic ($g_1 \neq g_2 \neq g_3$) and highly anisotropic (Δg 0.124−0.150) with g_1 close to the value observed for the free electron (g_e = 2.0023) (Figure 5b,c). The average g-values ($\langle g \rangle$) correspond closely to the isotropic g-values obtained from solution spectra. Anisotropic $A(^{95,97}Mo)$ hyperfine coupling was also observed, the largest coupling constant being A_3 followed by A_1, then A_2 (ca. 56 × 10^{-4}, 47 × 10^{-4}, and 31 × 10^{-4} cm^{-1}, respectively).

The EPR spectra are very similar to those reported for in situ generated oxosulfido-Mo(V) complexes, such as $[MoOS(L\text{-}N_2S_2)]^-$ [14−17] and $[Tp^xMoOSX]^-$ (Tp^{x-} = Tp^{iPr-}, Tp^{*-}; see Table 5),[62,63] the variations in g and A values being ascribed to differences in the coordination environments and attendant electronic structures. However, the spectra are distinctly different from those of monosulfido-Mo(V) complexes, where the sulfido ligand (rather than an oxo ligand) provides the strongest field ligand; these complexes exhibit EPR spectra with higher g_{iso} (∼1.90−1.96), smaller anisotropy ($\Delta g \approx 0.02$−0.1) and highly ligand-sensitive A_{iso} (ca. 46 × 10^{-4} cm^{-1} and 37 × 10^{-4} cm^{-1} for hard and soft ligand donors, respectively).[3,64,65] The spectra are also distinct from those reported for various dioxo-Mo(V) analogues, $[Tp^xMoO_2X]^-$; these complexes contain two strong field oxo ligands in a cis configuration and exhibit highly anisotropic spectra (Δg ca. 0.15−0.18) with lower g_{iso} (∼1.90−1.93) and marginally higher A_{iso} (∼40−45 × 10^{-4} cm^{-1}) values (especially when comparing analogous pairs of compounds).[53,54]

Table 5. Isotropic and Anisotropic EPR Parameters for Oxosulfido-Mo(V) Species[a]

cmpd number, Ar/other compds	g_{iso}	a_{iso}[b]	g_1	g_2	g_3	$\langle g \rangle$[c]	Δg[d]
1, Ph	1.925	40.3	1.999	1.924	1.849	1.925	0.149
2, $C_6H_4{}^sBu$-2	1.925	40.0	2.002	1.929	1.852	1.928	0.150
3, $C_6H_4{}^tBu$-2	1.923	40.3	1.997	1.931	1.869	1.932	0.128
4, $C_6H_4{}^tBu$-3	1.926	40.3	2.000	1.927	1.853	1.927	0.147
5, $C_6H_4{}^sBu$-4	1.926	43.1	2.001	1.929	1.853	1.927	0.148
6, C_6H_4Ph-4	1.927	43.1	2.002	1.924	1.855	1.928	0.147
7, $C_6H_3{}^tBu_2$-3,5	1.924	41.5	2.000	1.927	1.850	1.926	0.150
8, $C_6H_4CO_2Me$-2	1.924	41.5	2.002	1.926	1.853	1.927	0.147
9, $C_6H_4CO_2Et$-2	1.923	45.1	2.000	1.923	1.850	1.924	0.150
n.a., $C_6H_4CO_2Ph$-2	1.924	43.6	2.003	1.926	1.854	1.928	0.149
$[Tp^*MoOSCl]^-$[e]	1.937	37.4	2.010	1.930	1.874	1.938	0.136
$[Tp^*MoOS(NCS)]^-$[e]	1.937	36.6	2.010	1.930	1.874	1.938	0.136
$[Tp^*MoOS(SCH_2Ph)]^-$[e]	1.954	34.1	2.022	1.948	1.898	1.956	0.124
$[Tp^*MoOS(S_2PPr^i_2)]^-$[f]	1.938	43.5	2.013	1.933	1.880	1.941	0.133
$[Tp^*MoOS(S_2PPh_2)]^-$[f]	1.934	43.5	2.012	1.932	1.877	1.940	0.135
$[Tp^{iPr}MoOSCl]^-$[e]			2.011	1.932	1.868	1.937	0.143
$[Tp^{iPr}MoOSBr]^-$[e]			2.012	1.933	1.868	1.937	0.143
$[MoOS(L\text{-}N_2S_2)]^-$[g]			2.017	1.934	1.889	1.946	0.128
XnO-VR (xanthine)[h]			2.025	1.955	1.949	1.976	0.076

[a]Spectra of in situ generated title compounds in 10:1 THF/MeCN solution or frozen glass. [b]$a_{iso}(^{95,97}$ Mo) units: 10^{-4} cm^{-1}. [c]$\langle g \rangle = 1/3(g_1 + g_2 + g_3)$. [d]$\Delta g = g_1 - g_3$. [e]Reference 62. [f]Reference 63. [g]Reference 14. [h]Signal elicited by substrate xanthine. Very similar parameters pertain to the signal elicited by 2-hydroxy-6-methylpurine (ref 13).

DOI: 10.1021/acs.inorgchem.5b00708
Inorg. Chem. 2015, 54, 6386−6396

EPR is a valuable tool for studying paramagnetic metal centers in enzymes. Coupling interactions between unpaired electron(s) and the nonzero nuclear spins of the metal(s) (hyperfine coupling) and neighboring nuclei (superhyperfine coupling) provide information about the metal center, its first (ligand) and second coordination spheres, and its coordination geometry. Furthermore, spin−orbit coupling resulting from mixing of the ground and excited states modifies the g value of a pure spin state (g_e), thus providing information about the symmetry and electronic structure of the metal center.[66] Detailed analysis of the $\boldsymbol{g}$ and $\boldsymbol{A}$ tensor components provides additional information about the relative spin density (orbital splittings/mixing, wave function coefficients and degree of ligand covalency) of the metal center.

Many factors contribute to the $\boldsymbol{g}$ and $\boldsymbol{A}$ tensors of transition metal species and the computational analysis of bonding and simulation of EPR parameters in many-electron, low-symmetry, highly covalent species such as these is nontrivial. In a simplified, crystal field treatment for a d^1 distorted octahedral field, and anisotropy in $\boldsymbol{g}$ or deviation from g_e can be ascribed to spin−orbit coupling between the ground and excited states. Assuming a molecular coordinate system with z along the Mo═O vector and x and y close to the Mo⋯S and Mo−O_{Ar} vectors, the ground state orbital would be the π^* (Mo(d_{xy})−S(p_y)) SOMO in the xy plane perpendicular to the Mo−L vector of the strong field terminal oxo ligand, while the major contributors to the accessible excited states would be (in order of increasing energy) the d_{xz}, d_{yz}, and $d_{x^2-y^2}$ orbitals. Assuming close coincidence of g_{zz} with the Mo═O vector, the g values would, to first order and neglecting covalency, be given by eqs 1−3.

$$g_1 = g_e - 8\zeta/\Delta E_{x^2-y^2} \quad (1)$$

$$g_2 = g_e - 2\zeta/\Delta E_{yz} \quad (2)$$

$$g_3 = g_e - 2\zeta/\Delta E_{xz} \quad (3)$$

where $\Delta E_i = E_i - E_{xy}$ and ζ is the spin−orbit coupling constant for Mo^V (1030 cm^{-1}). Here, $g_1 \approx g_e$ due to the large energy gap between the d_{xy} and σ^* $d_{x^2-y^2}$ orbitals. The fact that $g_1 > g_e$ for XnO-VR and many of the model compounds in Table 5 is ascribed to the significant delocalization of spin density onto the terminal sulfido ligand. It is expected that the d_{xz} and d_{yz} orbitals would have similar energies but that the d_{yz} orbital will be destabilized by a π^* interaction with the O_{Ar} p_z orbital, thus increasing ΔE_{yz} relative to ΔE_{xz} accounting for the different $g_{2,3}$ values. Because of the significant destabilization of d_{xy} through the π^* interaction with the sulfido ligand, the energy gaps under discussion are expected to be very small.

Indeed, the electronic spectrum of **1** exhibits a weak, low-energy band centered at 1260 nm (7960 cm^{-1}, $\varepsilon \approx 70$ M^{-1} cm^{-1}), which is assigned to the formally forbidden $d_{xy} \rightarrow d_{xz,yz}$ transition. The band is much lower in energy than is typical of oxo-Mo(V) species (ca. 620 nm, 13 000−16 000 cm^{-1} [67,68]) due to the destabilization of the d_{xy} orbital (SOMO) through π interactions with the sulfido ligand. A first excited state of similar energy (relative to the ground state) was calculated for $[MoOS(L\text{-}N_2S_2)]^-$ by Peng et al.[69] Other sulfur-based ligand-to-metal charge transfer (LMCT) bands associated with the sulfido and phenolate ligands are observed at 520 nm (19 300 cm^{-1}, $\varepsilon \approx 400$ M^{-1} cm^{-1}) and 430 nm (23 400 cm^{-1}, $\varepsilon \approx 600$ M^{-1} cm^{-1}). Preliminary magnetic circular dichroism (MCD) studies suggest that multiple LMCT transitions, involving charge transfer from in- and out-of-plane combinations of the filled S and $O_{phenolate}$ p orbitals to semioccupied (d_{xy}) and virtual Mo d orbitals, contribute to these absorption bands.[70]

According to eqs 1−3, purely metal-based spin−orbit coupling terms make a net negative contribution to g values. However, as shown by Westmoreland and co-workers,[71,72] ligand-based terms make a large (dominant), positive contribution to $\boldsymbol{g}$ and can produce g values greater than g_e for highly covalent complexes. In the case of $[Mo^VOX_4]^-$ (X = F^- Cl^-, Br^-), as the complexes become more covalent in the plane perpendicular to the oxo ligand, specifically, F < Cl < Br, the contributions of ligand-based terms to $\boldsymbol{g}$ increases and $g_\parallel$ approaches and exceeds g_e (for X = Br^-, $g_\parallel = 2.090$). More recent studies support these findings and conclusions.[73]

In summary, g_1, g_2, and g_3 reflect spin−orbit coupling between the ground and accessible excited states and are likely to lie close to the Mo═O, Mo−O_{Ar}, and Mo⋯S vectors, respectively. Assessment of the influence of covalent interactions and low-energy LMCT transitions on the EPR spectra require more advanced spectroscopic[74,75] and theoretical[73,76−79] interrogation of the compounds, which are beyond the scope of the present paper.

There are striking similarities as well as differences in the EPR spectra of oxosulfido-Mo(V) compounds and XnO-VR (see Table 5). The most notable similarity is in the ^{33}S ($I = 3/2$) superhyperfine coupling observed for $[^{98}MoO^{33}S(L\text{-}N_2S_2)]^-$ and ^{33}S-labeled XnO-VR.[13] Indeed, the large, anisotropic coupling to ^{33}S ($a_{iso} = 11 \times 10^{-4}$ cm^{-1}) in both species provided the first compelling evidence for the presence of a highly covalent (S spin density ca. 35−38%), terminal sulfido ligand. Moreover, both species exhibit similarly high g_1 values, which approach or exceed g_e due to the effect of the remarkably high degree of covalency in the Mo⋯S and Mo−MPT moieties (vide infra).

However, the g_2 and g_3 values for the model compounds are consistently lower than those observed for XnO-VR. This may be ascribed to differences in the coordination numbers, geometries, and ligands present in available models compared to XnO-VR.[66] In particular, the highly covalent nature of the Mo−MPT pterin-dithiolene moiety present in the enzyme but absent from models is expected to contribute to an increase in g values, especially g_2 and g_3, relative to those of the less covalent, hard donor ligand model complexes. Many studies have corroborated the extensive covalency and noninnocence of metal dithiolene complexes,[80−82] including oxo-Mo(V) species relevant to molybdenum enzymes.[83,84] Delocalization of spin density from Mo onto the sulfur donor ligands of XnO-VR is consistent with the very low $a(^{95,97}Mo)$ (27.2×10^{-4} cm^{-1}) and high $a(^{33}S)$ (11×10^{-4} cm^{-1}) observed for this species.[13,14] Indeed, Westmoreland and co-workers have shown that metal−ligand covalency is the major contribution to the g anisotropy of oxo-Mo(V) species such as $[MoOX_4]^-$ (X^- = F^- Cl^-, Br^-);[71,72] it is likely that this situation extends to the title compounds and XnO-VR, where a single strong field oxo ligand dominates the ligand field.

Reactivity Studies. *Reactivity with Cyanide.* It is known that oxosulfido-Mo(VI) complexes, including $Tp^{iPr}MoOS(OAr)$, undergo cyanolysis to yield thiocyanate.[2,63,85] These reactions mimic the removal of the catalytically essential sulfido ligand from oxidized xanthine oxidase to produce *desulfo* xanthine oxidase and thiocyanate.[86]

EPR monitoring of the reactions of the title compounds with cyanide in chlorinated solvents revealed the abstraction of the

DOI: 10.1021/acs.inorgchem.5b00708
Inorg. Chem. 2015, 54, 6386−6396

terminal sulfido ligand as thiocyanate and the formation of $Tp^{iPr}MoOCl(OAr)$ (g = 1.939). In this case, the stability of the chloro complex prevents complicating reactions, but this is not the case in other solvents. For example, the same reaction in acetonitrile produces multiple species, including $Tp^{iPr}MoO(OSAr')$ (g = 1.956), $Tp^{iPr}MoO(OAr)_2$ (g = 1.942) and $[Tp^{iPr}MoO]_2(\mu\text{-}S_2)(\mu\text{-}O)$ (identified by ^{1}H NMR). Formation of $Tp^{iPr}MoO(OSAr')$ species is also supported by the isolation and structural characterization of $Tp^{iPr}MoO(OSC_6H_4\text{-}\kappa^2O,S)$ from the reaction of $Tp^{iPr}MoOS(OPh)$ and cyanide (see Supporting Information).

Reactions with Triphenylphosphine. Consistent with hard–soft acid–base theory and thermodynamic expectations, oxosulfido-Mo(VI) complexes react with phosphines to produce phosphine sulfides rather than phosphine oxides.[46] The reactions of $Tp^*MoOS(\kappa^1\text{-}S_2PR_2)$[63] and $Tp^{iPr}MoOS(OAr)$[87] complexes with PPh_3 to yield oxo-Mo(IV/V) complexes and SPPh are most pertinent to this paper. Reactions of the title compounds with PPh_3 in chlorinated solvents show similar reactivity to the cyanide reactions, with the formation of $Tp^{iPr}MoOCl(OAr)$ and $SPPh_3$ (identified with ^{31}P NMR and thin-layer chromatography). In acetonitrile, $SPPh_3$ is formed along with the multiple molybdenum species observed in the cyanide reactions. The reactions were complete is less than 5 min in both solvents.

Reactions with Copper Species. A potential synthetic route to models of the Mo/Cu carbon monoxide dehydrogenases (CODH),[88] involves the reaction of $[MoO(=S)]^{n+}$ complexes with copper species. Indeed, the reactions of the title compounds with $[Cu(MeCN)(Me_3tcn)]BF_4$ (Me_3tcn = 1,4,7-trimethyl-1,4,7-triazacyclononane) has provided excellent spectroscopic models for CODH.[89] Here, we describe reactions involving several other copper complexes.

The title complexes reacted instantaneously with $[Cu(MeCN)_4]BF_4$, Cu(MeCN)(β-diketiminate), and CuCl, leading to abstraction of the sulfur and the subsequent generation of various Mo-containing byproducts. In chlorinated solvents only one molybdenum species, $Tp^{iPr}MoOCl(OAr)$, was observed to form (detected by EPR). Reactions with 1 equiv of CuCl in nonchlorinated solvents also produced significant yields (ca. 40%) of $Tp^{iPr}MoOCl(OAr)$ along with unidentified species. Dinuclear Mo/Cu species were not observed to form. Reaction of **3** with $[Cu(MeCN)(ttcn)]BF_4$ in MeCN with subsequent cooling to −10 °C resulted in precipitation of light blue crystals of $Tp^{iPr}MoO(OC_6H_4{}^tBu\text{-}2)(MeCN)\cdot MeCN$, which were characterized by X-ray crystallography (see Supporting Information). This is consistent with solvolysis of any initially formed Mo–S–Cu complex, with the effective abstraction of the sulfur from the coordination sphere.

Implications of Reactivity Studies. Clearly, the terminal sulfido ligand, rather than the conserved oxo, phenolate, or Tp^{iPr-} ligands, is the center of reactivity in these compounds. The reactions are likely to be initiated by direct sulfur atom transfer although the participation of disproportionation or radical reactions cannot be discounted. Formal sulfur atom transfer, converting cyanide into thiocyanate, phosphines into phosphine sulfides, and Cu complexes into unidentified Cu/S species, would be predicted to form an oxo-Mo(III) species such as $[CoCp_2][Tp^{iPr}MoO(OAr)(MeCN)]$. However, oxo-Mo(III) species are extremely rare and highly reactive,[90] and facile oxidation prevents their isolation in the reactions above. The identity of the oxidant(s) has not been established, but the reagents and/or solvents are the most likely oxidants under anaerobic conditions. One-electron oxidation of the oxo-Mo(III) species would account for the frequent formation of blue $Tp^{iPr}MoO(OAr)(MeCN)$ in acetonitrile systems, while subsequent chlorine atom abstraction in chlorinated solvents and ligand exchange would account for the formation of stable oxo-Mo(V) complexes such as $Tp^{iPr}MoOCl(OAr)$ and $Tp^{iPr}MoO(OAr)_2$. The formation of $Tp^{iPr}MoO(OSAr')$ occurs slowly in the absence of sulfur atom donors but appears to be facilitated (in the case of more stable derivatives) or accelerated in the reactions above. Small amounts of dinuclear $[Tp^{iPr}MoO]_2(\mu\text{-}S_2)(\mu\text{-}O)$ are observed to form even in anaerobic solutions. Dimerization or disproportionation of $[Tp^{iPr}MoOS(OAr)]^-$ to form $[Tp^{iPr}MoOS(OAr)]_2{}^{2-}$ or $Tp^{iPr}MoOS(OAr)/[Tp^{iPr}MoOS(OAr)]^{2-}$ could also account for the formation of the products without the involvement of oxo-Mo(III) species. Additional studies are required to completely understand the rapid and complex reactions of these highly reactive species.

CONCLUSION

One-electron reduction of $Tp^{iPr}MoOS(OAr)$ with cobaltocene in toluene results in the precipitation of the oxosulfido-Mo(V) compounds $[CoCp_2][Tp^{iPr}MoOS(OAr)]$. These compounds constitute the first extended series of oxosulfido-Mo(V) complexes to be isolated and unambiguously characterized. The synthesis of $[MoOS(OAr)(dithiolene)]^{n-}$ complexes as models for Mo hydroxylases is a daunting task, one that has been thwarted by "downstream" reactions in these sterically unencumbered and reactive (noninnocent and redox-active) complexes.[9,10] In contrast, the bulky and relatively innocent nature of the Tp^{iPr-} and OAr^- coligands serve to stabilize the title compounds and facilitate their isolation. Significantly, the compounds are the first models for the key $[Mo^VOS(OAr)]$ moiety present in the "very rapid" form of xanthine oxidase (OAr^- = urate in XnO-VR). The crystal structure of **9**, the first reported for any oxosulfido-Mo(V) compound, revealed the presence of a short Mo---S bond (2.215(2) Å), consistent with results obtained from enzyme studies.[18,19,23] The properties of the compounds are very different than those of $PPh_4[MoOS(L\text{-}N_2S_2)]$, the only previously isolated oxosulfido-Mo(V) compound.[1] In particular, spectroscopic studies reveal that the frontier orbitals of oxosulfido-Mo(V) compounds are dominated by contributions from the Mo---S unit, with significant covalency and extensive spin delocalization across the whole unit. Accordingly, the reactivity of the compounds is focused on the terminal sulfido ligand, which is susceptible to abstraction by cyanide, phosphines, and copper complexes. A similar electronic structure in XnO-VR[13−15] is likely to facilitate the activation and oxidation of enzyme substrates and the conversion of XnO-VR to the "rapid type 1" form of the enzyme, proposed to contain an $[(MPT)Mo^VO(SH)(OR_{urate})]^-$ center.[11] Advanced spectroscopic and computational interrogation of these and related compounds have the potential to provide key results and insights informing enzyme behavior through electronic control of reactivity.

ASSOCIATED CONTENT

Supporting Information

Details of the synthesis and characterization of $Tp^{iPr}MoO(OSAr')$ complexes, descriptions of the crystal structures of $Tp^{iPr}MoO(OSC_6H_4)\cdot MeCN$ and $Tp^{iPr}MoO(OC_6H_4{}^tBu\text{-}2)(MeCN)\cdot MeCN$ and crystallographic data (for all structures)

DOI: 10.1021/acs.inorgchem.5b00708
Inorg. Chem. 2015, 54, 6386−6396

in CIF format. Tabulated isotropic and anisotropic *g*-values, ^{95,97}Mo hyperfine values, electrochemical data, bond distances and angles, ORTEP projection, additional references for the aforementioned compounds. The Supporting Information is available free of charge on the ACS Publications website at DOI: 10.1021/acs.inorgchem.5b00708.

AUTHOR INFORMATION

Corresponding Author

*E-mail: Charles.Young@latrobe.edu.au.

Notes

The authors declare no competing financial interest.
♦Deceased: 12 July, 2012.

ACKNOWLEDGMENTS

We thank Ms. N. Newey, Drs. H. H. Harris and S. Z. Knottenbelt, and Prof. M. L. Kirk for experimental assistance or helpful discussions. We gratefully acknowledge the financial support of the Albert Shimmins Memorial Fund, the Australian Nuclear Science and Technology Organization, the Australian Research Council, and the Petroleum Research Council (administered by the American Chemical Society). Portions of this research were performed at the SSRL, a Directorate of SLAC National Accelerator Laboratory, and the Office of Science User Facility operated for the U.S. Department of Energy Office of Science by Stanford University. SSRL is funded by the Department of Energy (DOE) BES, with further support by DOE OBER and the National Institutes of Health.

REFERENCES

(1) Singh, R.; Spence, J. T.; George, G. N.; Cramer, S. P. *Inorg. Chem.* **1989**, *28*, 8−10.
(2) Smith, P. D.; Slizys, D. A.; George, G. N.; Young, C. G. *J. Am. Chem. Soc.* **2000**, *122*, 2946−2947.
(3) Young, C. G.; Gable, R. W.; Hill, J. P.; George, G. N. *Eur. J. Inorg. Chem.* **2001**, 2227−2231.
(4) Doonan, C. J.; Nielsen, D. J.; Smith, P. D.; White, J. W.; George, G. N.; Young, C. G. *J. Am. Chem. Soc.* **2006**, *128*, 305−316.
(5) Doonan, C. J.; Rubie, N. D.; Peariso, K.; Harris, H. H.; Knottenbelt, S. Z.; George, G. N.; Young, C. G.; Kirk, M. L. *J. Am. Chem. Soc.* **2008**, *130*, 55−65.
(6) Young, C. G. In *Biomimetic Oxidations Catalyzed by Transition Metal Complexes;* Meunier, B., Ed.; Imperial College Press: London, U.K., 2000; pp 415−459.
(7) Young, C. G. In *Comprehensive Coordination Chemistry II;* McCleverty, J. A., Meyer, T. J., Eds.; Elsevier-Pergamon: Amsterdam, 2004; Vol. *4*, Chapter 4.7, pp 415−527.
(8) Lizano, A. C.; Munchhof, M. G.; Haub, E. K.; Noble, M. E. *J. Am. Chem. Soc.* **1991**, *113*, 9204−9210.
(9) Young, C. G. *J. Biol. Inorg. Chem.* **1997**, *2*, 810−816.
(10) Young, C. G. *J. Inorg. Biochem.* **2007**, *101*, 1562−1585.
(11) Hille, R. *Biol. Mag. Res.* **2010**, *29*, 91−120.
(12) Hille, R.; Hall, J.; Basu, P. *Chem. Rev.* **2014**, *114*, 3963−4038.
(13) George, G. N.; Bray, R. C. *Biochemistry* **1988**, *27*, 3603−3609.
(14) Wilson, G. L.; Greenwood, R. J.; Pilbrow, J. R.; Spence, J. T.; Wedd, A. G. *J. Am. Chem. Soc.* **1991**, *113*, 6803−6812 and references cited therein.
(15) Greenwood, R. J.; Wilson, G. L.; Pilbrow, J. R.; Wedd, A. G. *J. Am. Chem. Soc.* **1993**, *115*, 5385−5392.
(16) Dowerah, D.; Spence, J. T.; Singh, R.; Wedd, A. G.; Wilson, G. L.; Farchione, F.; Enemark, J. H.; Kristofzski, J.; Bruck, M. *J. Am. Chem. Soc.* **1987**, *109*, 5655−5665.
(17) Wilson, G. L.; Kony, M.; Tiekink, E. R. T.; Pilbrow, J. R.; Spence, J. T.; Wedd, A. G. *J. Am. Chem. Soc.* **1988**, *110*, 6923−6925.
(18) Bordas, J.; Bray, R. C.; Garner, C. D.; Gutteridge, S.; Hasnain, S. S. *Biochem. J.* **1980**, *191*, 499−508.
(19) Cramer, S. P.; Wahl, R.; Rajagopalan, K. V. *J. Am. Chem. Soc.* **1981**, *103*, 7721−7727.
(20) Lorigan, G. A.; Britt, R. D.; Kim, J. H.; Hille, R. *Biochim. Biophys. Acta* **1994**, *1185*, 284−294.
(21) Jones, R. M.; Inscore, F. E.; Hille, R.; Kirk, M. L. *Inorg. Chem.* **1999**, *38*, 4963−4970.
(22) Manikandan, P.; Choi, E.-Y.; Hille, R.; Hoffman, B. M. *J. Am. Chem. Soc.* **2001**, *123*, 2658−2663.
(23) Pauff, J. M.; Zhang, J.; Bell, C. E.; Hille, R. *J. Biol. Chem.* **2008**, *283*, 4818−4824.
(24) Voityuk, A. A.; Albert, K.; Romão, M. J.; Huber, R.; Rösch, N. *Inorg. Chem.* **1998**, *37*, 176−180.
(25) Ilich, P.; Hille, R. *J. Phys. Chem. B* **1999**, *103*, 5406−5412.
(26) Bayse, C. A. *Inorg. Chem.* **2006**, *45*, 2199−2202.
(27) Ng, V. W. L.; White, J. M.; Young, C. G. *J. Am. Chem. Soc.* **2013**, *135*, 7106−7109.
(28) Ng, V. W. L.; Taylor, M. K.; Young, C. G. *Inorg. Chem.* **2012**, *51*, 3202−3211.
(29) Hetherington, A.; Levason, W.; Spicer, M. D. *Polyhedron* **1990**, *9*, 1609−1612.
(30) Spencer, D. J. E.; Reynolds, A. M.; Holland, P. L.; Jazdzewski, B. A.; Duboc-Toia, C.; Le Pape, L.; Yokota, S.; Tachi, Y.; Itoh, S.; Tolman, W. B. *Inorg. Chem.* **2002**, *41*, 6307−6321.
(31) Hirsch, J.; DeBeer George, S.; Solomon, E. I.; Hedman, B.; Hodgson, K. O.; Burstyn, J. N. *Inorg. Chem.* **2001**, *40*, 2439−2441.
(32) *WinEPR-SimFonia;* Bruker Analytische Messtechnik GmbH: Karlsruhe, Germany, 1996.
(33) Connelly, N. G.; Gieger, W. E. *Chem. Rev.* **1996**, *96*, 877−910.
(34) Sörbo, B. *Biochim. Biophys. Acta* **1957**, *24*, 324−329.
(35) Sheldrick, G. M. *SHELXS-97 Program for Crystal Structure Solution;* University of Göttingen: Germany, 1993.
(36) Sheldrick, G. M. *SHELXL-97 Program for Crystal Structure Refinement;* University of Göttingen: Germany, 1997.
(37) Farrugia, L. J. *J. Appl. Crystallogr.* **1997**, *30*, 565.
(38) Bruno, I. J.; Cole, J. C.; Edgington, P. R.; Kessler, M.; Macrae, C. F.; McCabe, P.; Pearson, J.; Taylor, R. *Acta Crystallogr., Sect. B* **2002**, *58*, 389−397.
(39) Macrae, C. F.; Edgington, P. R.; McCabe, P.; Pidcock, E.; Shields, G. P.; Taylor, R.; Towler, M.; van de Streek, J. *J. Appl. Crystallogr.* **2006**, *39*, 453−457.
(40) Song, I.; Rickett, B.; Janavicius, P.; Payer, J. H.; Antonio, M. R. *Nucl. Instrum. Methods Phys. Res., Sect. A* **1995**, *360*, 634−641.
(41) Sekiyama, H.; Kosugi, N.; Kuroda, H.; Ohta, T. *Bull. Chem. Soc. Jpn.* **1986**, *59*, 575−579.
(42) Pickering, I.; George, G. N. *Inorg. Chem.* **1995**, *34*, 3142−3152.
(43) Hartley, D.; Ware, M. J. *J. Chem. Soc. A* **1969**, 138−142.
(44) Millar, A. J.; Doonan, C. J.; Laughlin, L. J.; Tiekink, E. R. T.; Young, C. G. *Inorg. Chim. Acta* **2002**, *337*, 393−406.
(45) Faller, J. W.; Ma, Y. *Organometallics* **1989**, *8*, 609−612.
(46) Thapper, A.; Donahue, J. P.; Musgrave, K. B.; Willer, M. W.; Nordlander, E.; Hedman, B.; Hodgson, K. O.; Holm, R. H. *Inorg. Chem.* **1999**, *38*, 4104−4114.
(47) Miao, M.; Willer, M. W.; Holm, R. H. *Inorg. Chem.* **2000**, *39*, 2843−2849.
(48) Eagle, A. A.; Tiekink, E. R. T.; George, G. N.; Young, C. G. *Inorg. Chem.* **2001**, *40*, 4563−4573.
(49) Orpen, A. G.; Brammer, L.; Allen, F. H.; Kennard, O.; Watson, D. G.; Taylor, R. *J. Chem. Soc., Dalton Trans.* **1989**, S1−S83.
(50) Trnka, T. M.; Parkin, G. *Polyhedron* **1997**, *16*, 1031−1045.
(51) Czernuszewicz, R. S.; Spiro, T. G. In *Inorganic Electronic Structure and Spectroscopy;* Solomon, E. I., Lever, A. B. P., Eds.; Wiley: New York, 1999; Vol. *1*, pp 353−441.
(52) Badger, R. M. *J. Chem. Phys.* **1935**, *3*, 710−714.
(53) Xiao, Z.; Gable, R. W.; Wedd, A. G.; Young, C. G. *J. Am. Chem. Soc.* **1996**, *118*, 2912−2921.
(54) Ng, V. W. L.; Taylor, M. K.; White, J. M.; Young, C. G. *Inorg. Chem.* **2010**, *49*, 9460−9469.

DOI: 10.1021/acs.inorgchem.5b00708
Inorg. Chem. 2015, 54, 6386−6396

(55) Rowland, R. S.; Taylor, R. *J. Phys. Chem.* **1996**, *100*, 7384−7391.
(56) Desiraju, G. R. *Acc. Chem. Res.* **1991**, *24*, 290−296.
(57) Desiraju, G. R. *Acc. Chem. Res.* **1996**, *29*, 441−449.
(58) Braga, D.; Grepioni, F.; Desiraju, G. R. *Chem. Rev.* **1998**, *98*, 1375−1406.
(59) Diana, E.; Stanghellini, P. L. *J. Am. Chem. Soc.* **2004**, *126*, 7418−7419.
(60) Shadle, S. E.; Penner-Hahn, J. E.; Schugar, H. J.; Hedman, B.; Hodgson, K. O.; Solomon, E. I. *J. Am. Chem. Soc.* **1993**, *115*, 767−776.
(61) Eagle, A. A.; George, G. N.; Tiekink, E. R. T.; Young, C. G. *Inorg. Chem.* **1997**, *36*, 472−479.
(62) Xiao, Z.; Bruck, M. A.; Doyle, C.; Enemark, J. H.; Grittini, C.; Gable, R. W.; Wedd, A. G.; Young, C. G. *Inorg. Chem.* **1995**, *34*, 5950−5962; *Erratum: ibid.* **1996**, *35*, 5752.
(63) Laughlin, L. J.; Eagle, A. A.; George, G. N.; Tiekink, E. R. T.; Young, C. G. *Inorg. Chem.* **2007**, *46*, 939−948.
(64) Young, C. G.; Enemark, J. H.; Collison, D.; Mabbs, F. E. *Inorg. Chem.* **1987**, *26*, 2925−2927.
(65) Hanson, G. R.; Wilson, G. L.; Bailey, T. D.; Pilbrow, J. R.; Wedd, A. G. *J. Am. Chem. Soc.* **1987**, *109*, 2609−2616.
(66) Mabbs, F. E.; Collison, D. *Electron Paramagnetic Resonance of d Transition Metal Compounds;* Elsevier: Amsterdam, 1992.
(67) Carducci, M. D.; Brown, C.; Solomon, E. I.; Enemark, J. H. *J. Am. Chem. Soc.* **1994**, *116*, 11856−11868.
(68) McMaster, J.; Carducci, M. D.; Yang, Y.-S.; Solomon, E. I.; Enemark, J. H. *Inorg. Chem.* **2001**, *40*, 687−702.
(69) Peng, G.; Nichols, J.; McCullough, E. A., Jr.; Spence, J. T. *Inorg. Chem.* **1994**, *33*, 2857−2864.
(70) Rubie, N. D.; Peariso, K.; Knottenbelt, S. Z.; Kirk, M. L. Personal communication of unpublished results, 2014.
(71) Balagopalakrishna, C.; Kimbrough, J. T.; Westmoreland, T. D. *Inorg. Chem.* **1996**, *35*, 7758−7768.
(72) Swann, J.; Westmoreland, T. D. *Inorg. Chem.* **1997**, *36*, 5348−5357.
(73) Hadt, R. G.; Nemykin, V. N.; Olsen, J. G.; Basu, P. *Phys. Chem. Chem. Phys.* **2009**, *11*, 10377−10384 and references cited therein.
(74) Cosper, M. M.; Neese, F.; Astashkin, A. V.; Carducci, M. D.; Raitsimring, A. M.; Enemark, J. H. *Inorg. Chem.* **2005**, *44*, 1290−1301.
(75) Drew, S. C.; Hill, J. P.; Lane, I.; Hanson, G. R.; Gable, R. W.; Young, C. G. *Inorg. Chem.* **2007**, 2373−2387.
(76) Kaupp, M.; Buehl, M.; Malkin, V. G. *Calculation of NMR and EPR Parameters: Theory and Applications;* Wiley-VCH: Weinheim, Germany, 2004.
(77) Hrobárik, H.; Repiský, M.; Komorovský, S.; Hrobáriková, V.; Kaupp, M. *Theor. Chem. Acc.* **2011**, *129*, 715−725 and references cited therein.
(78) Fritscher, J.; Hrobárik, P.; Kaupp, M. *Inorg. Chem.* **2007**, *46*, 8146−8161.
(79) Drew, S. C.; Young, C. G.; Hanson, G. R. *Inorg. Chem.* **2007**, *46*, 2388−2397.
(80) Samuel, P. P.; Horn, S.; Döring, A.; Havelius, K. G. V.; Reschke, S.; Leimkühler, S.; Haumann, M.; Schulzke, C. *Eur. J. Inorg. Chem.* **2011**, 4387−4399.
(81) Sproules, S.; Wieghardt, K. *Coord. Chem. Rev.* **2011**, *255*, 837−860.
(82) Sproules, S. *Prog. Inorg. Chem.* **2014**, *58*, 1−144.
(83) Inscore, F. E.; McNaughton, R.; Westcott, B. L.; Helton, M. E.; Jones, R.; Dhawan, I. K.; Enemark, J. H.; Kirk, M. L. *Inorg. Chem.* **1999**, *38*, 1401−1410.
(84) Joshi, H. K.; Cooney, J. J. A.; Inscore, F. E.; Gruhn, N. E.; Lichtenberger, D. L.; Enemark, J. H. *Proc. Nat. Acad. Sci., U.S.A.* **2003**, *100*, 3719−3724.
(85) Traill, P. R.; Tiekink, E. R. T.; O'Connor, M. J.; Snow, M. R.; Wedd, A. G. *Aust. J. Chem.* **1986**, *39*, 1287−1295.
(86) Coughlan, M. P.; Johnson, J. L.; Rajagopalan, K. V. *J. Biol. Chem.* **1980**, *255*, 2694−2699.
(87) Doonan, C. J. *Novel cis-Oxo-sulfido-molybdenum Complexes Which Model Molybdenum Hydroxylases*, Ph.D. Dissertation, University of Melbourne, 2004.
(88) Hille, R.; Dingwall, S.; Wilcoxen, J. *J. Biol. Inorg. Chem.* **2015**, *20*, 243−251.
(89) Gourlay, C.; Nielsen, D. J.; White, J. M.; Knottenbelt, S. Z.; Kirk, M. L.; Young, C. G. *J. Am. Chem. Soc.* **2006**, *128*, 2164−2165.
(90) Behrens, A.; Behrens, U.; Nordlander, E.; Bader, C.; Rehder, D. *Inorg. Chim. Acta* **2005**, *358*, 1970−1974.

DOI: 10.1021/acs.inorgchem.5b00708
Inorg. Chem. 2015, 54, 6386−6396